# Seismicity Remotely Triggered by the Magnitude 7.3 Landers, California, Earthquake

D. P. Hill, P. A. Reasenberg, A. Michael, W. J. Arabaz, G. Beroza, D. Brumbaugh, J. N. Brune, R. Castro, S. Davis, D. dePolo, W. L. Ellsworth, J. Gomberg, S. Harmsen, L. House, S. M. Jackson, M. J. S. Johnston, L. Jones, R. Keller, S. Malone, L. Munguia, S. Nava, J. C. Pechmann, A. Sanford, R. W. Simpson, R. B. Smith, M. Stark, M. Stickney, A. Vidal, S. Walter, V. Wong, J. Zollweg

The magnitude 7.3 Landers earthquake of 28 June 1992 triggered a remarkably sudden and widespread increase in earthquake activity across much of the western United States. The triggered earthquakes, which occurred at distances up to 1250 kilometers (17 source dimensions) from the Landers mainshock, were confined to areas of persistent seismicity and strike-slip to normal faulting. Many of the triggered areas also are sites of geothermal and recent volcanic activity. Static stress changes calculated for elastic models of the earthquake appear to be too small to have caused the triggering. The most promising explanations involve nonlinear interactions between large dynamic strains accompanying seismic waves from the mainshock and crustal fluids (perhaps including crustal magma).

At 1157 UT (04:57 PDT) on 28 June 1992, southern California was rocked by the magnitude (**M**) 7.3 Landers earthquake, the largest earthquake to strike the region in 40 years (*1*). The earthquake resulted from a northward propagating rupture producing up to 6 m of right-lateral, strike-slip displacement on a series of faults extending over 70 km north-northwest into the Mojave desert from the epicenter 5 km southwest of the town of Landers (Fig. 1). Within minutes after the Landers mainshock, earthquake activity abruptly increased at widely scattered sites across the western United States (*2*).

That earthquake activity can be triggered by a nearby source is well known. Aftershocks of large and moderate earthquakes commonly occur at distances of one or two source dimensions from a mainshock (*3*). Seismicity induced by human activities (which include the underground detonation of nuclear explosions, filling or emptying of water reservoirs, injecting and extracting fluids in deep boreholes, and mining) is usually confined to an area within a few tens of kilometers or less of the inducing source (*4*). In marked contrast, the widespread surge in post-Landers seismic activity extended over 1250 km (17 source dimensions) from the mainshock.

This abrupt, widespread, and unexpected seismicity increase challenges a long-standing skepticism regarding the reality of triggered seismic activity at great distances from an earthquake. This skepticism has its roots, in part, in the uncertain significance associated with an increase in earthquake activity at a solitary, remote site after a large earthquake, and, in part, in the lack of a plausible physical model for remote triggering. In particular, Earth models based on linear elasticity, which have been successful in explaining a vast range of seismological phenomena, seem incapable of accounting for triggered seismicity beyond a few source dimensions of an earthquake rupture (*5*). The simultaneous increase in seismic activity at many remote sites following the Landers earthquake thus forces consideration of an expanded range of models that include nonlinear interactions.

In this article we document the spatial distribution and temporal evolution of the seismic activity that followed the Landers mainshock and the tectonic settings in which the activity occurred. We argue that this activity is not explained by random coincidence and comment on evidence for remote triggering by other major ($M \geq 7$) earthquakes. We conclude by exploring some possible physical processes that might explain remote triggering.

**Distribution and nature of triggered seismicity.** Recognition of remotely trig-

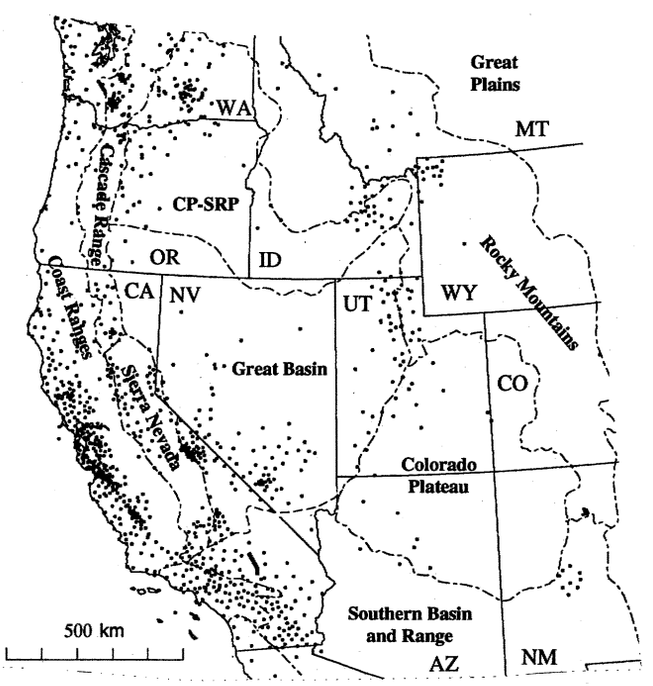


**Fig. 1.** Map showing seismograph stations in the western United States and Mexico used in this study (*2*). The Landers mainshock rupture is shown by heavy solid line. Major physiographic provinces are outlined by dashed lines. Abbreviation: CP-SRP, Columbia Plateau-Snake River Plain.

D. P. Hill, P. A. Reasenberg, A. Michael, W. L. Ellsworth, M. J. S. Johnston, R. W. Simpson, and S. Walter are at the U.S. Geological Survey, Menlo Park, CA 94025. W. J. Arabaz, S. Nava, J. C. Pechmann, and R. B. Smith are at the University of Utah, Salt Lake City, UT 84112. G. Beroza is at Stanford University, Stanford, CA 94305. D. Brumbaugh is at Northern Arizona University, Flagstaff, AZ 86011. J. N. Brune and D. dePolo are at the University of Nevada, Reno, NV 89557. R. Castro, L. Munguia, A. Vidal, and V. Wong are at CICESE, Ensenada, Mexico. S. Davis is at the University of Texas, Austin, TX 78712. J. Gomberg and S. Harmsen are at the U.S. Geological Survey, Golden, CO. L. House is at Los Alamos National Laboratories, Los Alamos, NM 87545. S. M. Jackson is at Idaho National Engineering Laboratory, Idaho Falls, ID 83401. L. Jones is at the U.S. Geological Survey, Pasadena, CA. R. Keller is at the University of Texas at El Paso, El Paso, TX 79968. S. Malone is at the University of Washington, Seattle, WA 98195. A. Sanford is at the New Mexico Institute of Mining and Technology, Socorro, NM 87801. M. Stark is at Unocal Corporation, Santa Rosa, CA. M. Stickney is at the Montana Bureau of Mines and Geology, Butte, MT 59701. J. Zollweg is at Boise State University, Boise, ID 83725.

gered seismicity depends critically on the distribution of seismic networks. Because the networks operating in the western United States and northern Mexico (Fig. 1) do not provide spatially uniform coverage and their detection thresholds vary, recognition of seismicity triggered by the Landers event is probably incomplete. For example, a sequence of $M < 2$ earthquakes triggered in southeastern Oregon or southern Arizona would not be detected by any of the operating networks. Furthermore, before the late 1970s many of the present networks were sparse or nonexistent. Had the Landers earthquake occurred before then, the chances are poor that triggered activity would have been recognized.

The most dramatic increase in earthquake activity occurred in the Landers aftershock zone within 100 km of the rupture (Fig. 2), which we do not consider further (6). We also do not consider possible triggered activity in southern California between the Garlock fault and the international border, for which a complete earthquake catalog is not yet available for the period of interest. There are, however, two candidates for triggered activity in southern California: A cluster beneath Pasadena (PA in Fig. 2) 60 km west of the aftershock ellipse that included a $M = 3.9$ event on 29 June and a lineation of earthquakes along and east of the White Wolf fault (source of the $\mathbf{M} = 7.5$ Kern County earthquake of 1952; WW and K in Fig. 2).

North of the Garlock fault, post-Landers earthquake activity was concentrated within a belt of persistent seismicity and Holocene faulting that extends north-northwest from the southern margin of the Great Basin (7) as far north as the southern Cascade volcanoes in northern California. Within this region, triggered activity was primarily concentrated along the boundary zone between the Sierra Nevada and Great Basin (SNGBZ), although some activity occurred in more isolated sites, each also with a history of persistent seismic activity (Figs. 2 to 7). Particularly noteworthy aspects of the triggered sites include: (i) all sites of (recognized) remote triggering are north of the Landers mainshock and (ii) all sites show strike-slip to normal faulting (implying a horizontal orientation for the least principal stress). Many sites of persistent seismicity north of Landers did not respond with triggered seismicity, however. Notably, active sections of the San Andreas fault system in central and northern California, the Intermountain seismic belt in central and northern Utah, and the central Nevada belt (8) showed no response. Many sites of remotely triggered activity are also closely associated with areas of geothermal activity or young volcanism (last 1 million years). Sites of triggered activity lacking geothermal activity or young volcanism are concentrated just east of the California-Nevada border from the eastern side of the White Mountains to near Lake Tahoe. Triggered sites in southern Nevada (Little Skull Mountain) and western Utah (Cedar City) are not near geothermal systems but are within 20 km of Pleistocene (≤1 million year old) basaltic vents (9). Only a few of the many seismically active geothermal and young volcanic systems in the region, however, responded with triggered activity. The seismogenic Brawley and Cerro Prieto geothermal areas in the Imperial Valley–Salton Trough south of Landers (distance from Landers epicenter $\Delta = 150$ to 250 km;

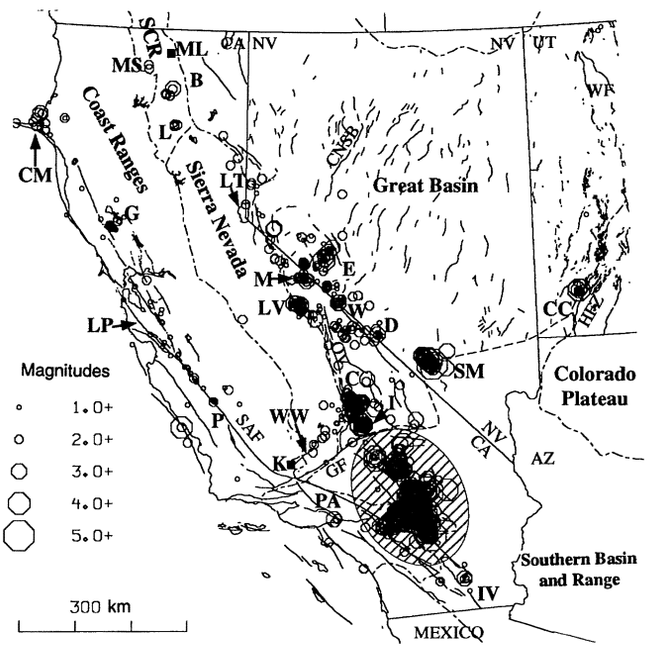


**Fig. 2.** Map showing earthquake activity detected by the combined seismic network in the 10 days immediately after the Landers earthquake. Major physiographic provinces are outlined by dashed lines. Faults with quaternary movement are shown by solid lines. Shaded ellipse extending approximately 100 km beyond the Landers rupture represents the aftershock zone. Abbreviations: AZ, Arizona; B, Burney; C, Coso Hot Springs; CA, California; CC, Cedar City, Utah; CM, 1992 Cape Mendocino earthquake epicenter; CNSB, central Nevada seismic belt; D, Death Valley; E, Excelsior Mountains; G, Geysers; GF, Garlock fault; HFZ, Hurricane fault zone; I, Indian Wells Valley; IV, Imperial Valley; K, 1952 Kern County earthquake epicenter; LP, 1989 Loma Prieta earthquake epicenter; L, Lassen Peak; LV, Long Valley caldera; LT, Lake Tahoe; M, Mono Basin; ML, Medicine Lake caldera; MS, Mount Shasta; NV, Nevada; OV, Owens Valley; P, Parkfield; PA, Pasadena; SAF, San Andreas fault zone; SCR, Southern Cascade Range; SM, Little Skull Mountain; UT, Utah; W, White Mountains; WF, Wasatch fault zone; WW, White Wolf fault.

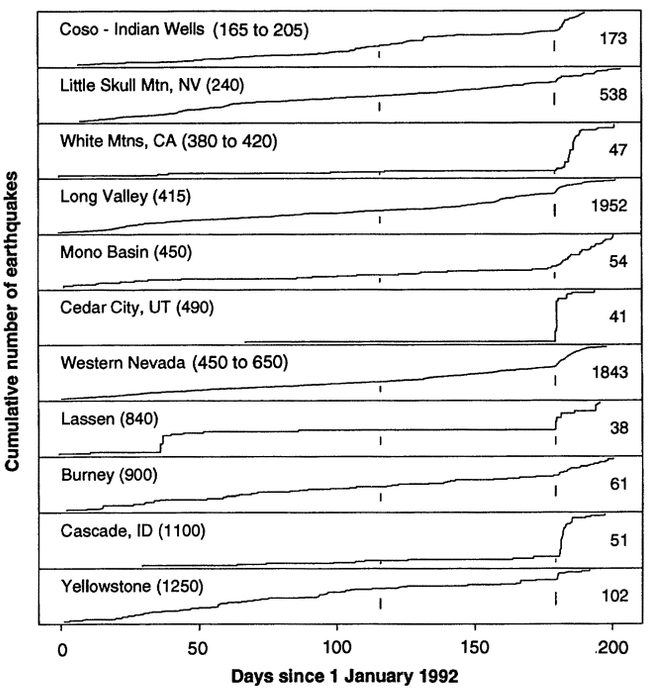


**Fig. 3.** Cumulative number of locatable earthquakes in selected zones, beginning 1 January 1992. Numbers in parentheses are distances (in kilometers) from Landers earthquake. Total number of earthquakes in each zone is shown at right. Vertical lines mark times of the 25 April 1992 Petrolia (Cape Mendocino) ($\mathbf{M} = 7.1$) and Landers ($\mathbf{M} = 7.3$) earthquakes.

IV in Fig. 2) are particularly notable for the absence of triggered activity (*10*).

Both the maximum magnitude and the total seismic moment of the remotely triggered earthquakes decreased with distance from the Landers epicenter (Table 1 and Fig. 4). The largest triggered earthquake was a **M** = 5.6 event beneath Little Skull Mountain in southern Nevada (Δ = 240 km) on 29 June at 1014 UT located approximately 20 km east of a group of basaltic vents that erupted sometime between 0.02 and 1.0 million years ago (Ma) (9). This earthquake, which had an oblique normal mechanism with a northwest-southeast T-axis (extension direction), was preceded by at least 19 smaller events within 100 km of Little Skull Mountain beginning as soon as 91 min after the Landers mainshock (even earlier events could have been obscured by seismic waves generated by the intense Landers aftershock activity). It was the largest earthquake to occur in this section of the southern Great Basin since 1868.

Triggered activity along the eastern margin of the Sierra Nevada and adjacent sections of western Nevada was concentrated in scattered clusters from the Indian Wells Valley–Coso area north of the Garlock fault (Δ = 165 to 205 km) to near Lake Tahoe (Δ = 500 km). The SNGBZ is marked by numerous Quaternary basaltic and rhyolitic volcanic centers and geothermal areas and has been a persistent source of moderate-to-large earthquakes throughout historic time, which dates from the mid-1800s (*11*). Long Valley caldera has been the most active area within the SNGBZ during the last decade and has had frequent earthquake swarms and over 0.5 m of ground uplift. It is the site of the most recent volcanism within the SNGBZ; the most recent eruptions were just 500 to 600 years ago along the Inyo-Mono craters volcanic chain (*12*). The triggered seismicity within the SNGBZ, which included numerous events between M = 3 and 4, coincides closely with the locations and depths of earthquakes located there during the past several decades. Specific areas of triggered activity within this region include (see Fig. 2): (i) a 60-km-long, north-northwest-trending lineation along the base of the Sierra Nevada from Indian Wells Valley to the vicinity of Coso Hot Springs; (ii) a diffuse cluster cutting westward from the California-Nevada border near 37°N across the northern end of Death Valley through the Inyo Mountains into Owens Valley; (iii) a dense cluster concentrated in the south moat of Long Valley caldera, including three clusters along the California-Nevada border, two east of Long Valley along the east margin of the White Mountains, and one north of Long Valley in the Mono Basin; (iv) a cluster elongated to the northeast in the Excelsior Mountains (E) in western Nevada; and (v) a diffuse lineation along the

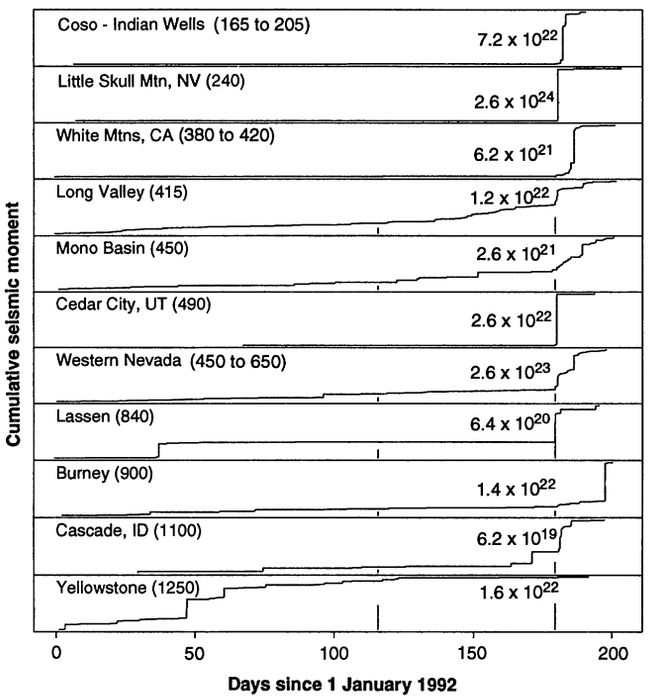


**Fig. 4.** Cumulative seismic moment in selected zones, beginning 1 January 1992. Numbers in parentheses are distances (in kilometers) from Landers earthquake. Total seismic moment (in dyne-cm) for each zone is shown at right. Vertical lines mark times of the Petrolia (Cape Mendocino) (**M** = 7.1) and Landers (**M** = 7.3) earthquakes.

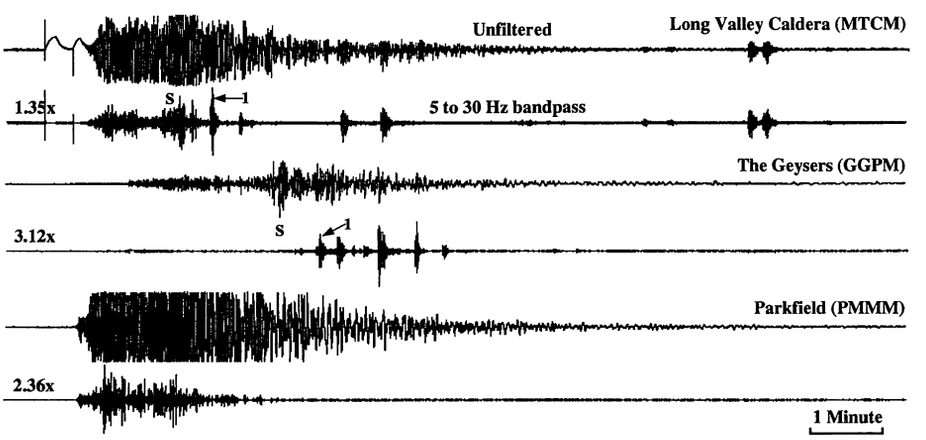


**Fig. 5.** Unfiltered and filtered vertical-component, ground-velocity seismograms from low-gain Calnet stations at Long Valley caldera, the Geysers geothermal area, and Parkfield. Number next to filtered trace indicates its magnification relative to corresponding unfiltered trace. S indicates arrival of Landers S wave and 1 indicates first identified triggered event at each site.

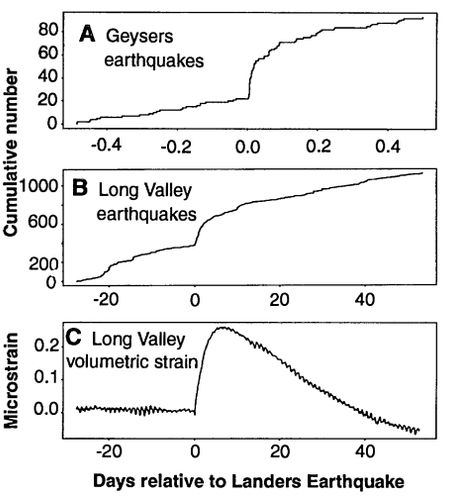


**Fig. 6.** Response of seismicity and strain to the Landers earthquake. (**A**) Cumulative number of earthquakes detected at the Geysers geothermal area in a 24-hour period surrounding the Landers earthquake. (**B**) Cumulative number of earthquakes detected at Long Valley caldera between 1 June and 20 August 1992. (**C**) Dilatational strain recorded at Devils Postpile, located approximately 10 km west of the triggered seismicity in Long Valley caldera, during the same interval. Increasing values correspond to increasing compression. Tidal strains and a secular dilatational strain rate of −0.007 microstrain per day have been removed, but a residual tidal strain signal remains. The transient dynamic Landers signal (6.4 microstrain) is not shown on this record.

eastern margin of the Sierra Nevada between Bridgeport and Lake Tahoe.

The triggered swarm near Cedar City in southwestern Utah ($\Delta$ = 490 km) included more than 60 earthquakes (at least seven of which were felt locally) within the Hurricane fault zone, the principal zone of bounding faults between the Colorado Plateau and the eastern Great Basin. The earthquakes were all within 15 to 20 km of Quaternary basalt flows with dates of 1.0 to 1.2 Ma (9). No other sites along the seismically active, eastern margin of the Great Basin [the Intermountain seismic belt (*13*)] showed evidence of triggered activity.

Beyond 600 km, isolated clusters of less intense activity occurred in the Geysers geothermal area ($\Delta$ = 740 km), the southern Cascade range ($\Delta$ = 840 to 900 km), Yellowstone National Park ($\Delta$ = 1250 km), and western Idaho ($\Delta$ = 1100 km). The triggered activity at the Geysers consisted of a surge of $M < 1$ earthquakes that began 30 s after the arrival of the Landers S wave and decayed to background levels 3 hours later (Fig. 6A). This is the only triggered activity recognized within the northern San Andreas fault system. In the southern Cascade Range, earthquake activity increased at Lassen Peak, Medicine Lake caldera, and near Burney (an area covered by Quaternary lava flows). Triggered seismicity near Cascade, Idaho, was located in the western part of the Idaho batholith (see Fig. 7) some 15 km west of the nearest hot spring. The most distant candidate for activity triggered by the Landers mainshock occurred in a small cluster 15 km northwest of Yellowstone caldera within Yellowstone National Park (*14*) (see Fig. 7).

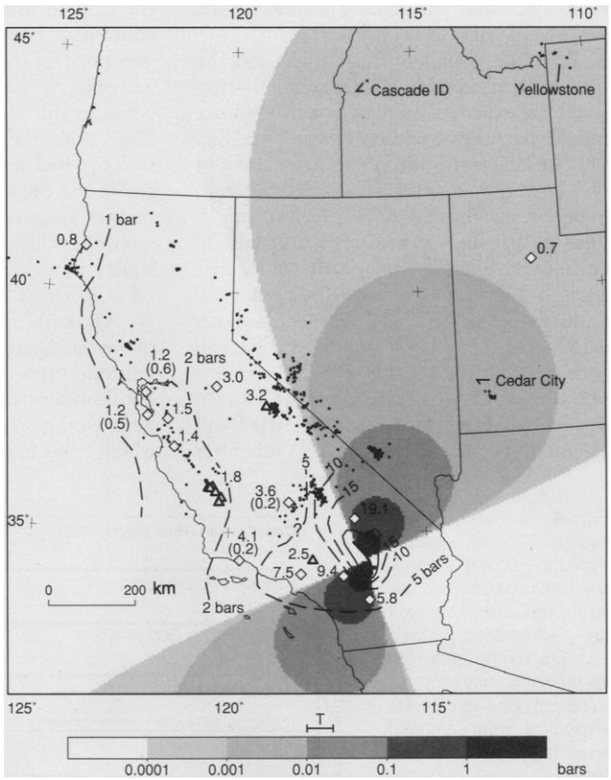


**Fig. 7.** Map showing static mean stress change and peak dynamic stress in bars for the Landers mainshock at mid-crustal depth together with the first 10 days of post-Landers seismicity. The static mean stress change was calculated for an elastic half-space using the three-dimensional boundary element subroutines of Okada (*34*) and a model for the Landers rupture based on Caltech Terrascope data and surface slip observations (*1*). **T** indicates typical range of tidal stresses. Shading shows the expansional quadrants; the compressional quadrants can be filled in by 90° rotation of the shaded pattern and a sign change. (Maximum static shear stress changes resolved onto vertical planes based on the same model are listed in Table 1.) Numbers indicate peak dynamic mean stress from borehole dilatometer data (triangles) and peak dynamic shear stress from regional digital seismic stations (diamonds). Value at Parkfield (1.8) is mean of six dilatometer observations. Parenthetic numbers are peak dynamic stresses for the **M** ≈ 7.1 Petrolia (Cape Mendocino) earthquake, shown for comparison. Contours suggest general pattern of peak dynamic stresses from the Landers mainshock without distinguishing between mean and shear stresses.

**Temporal patterns in triggered activity.** Establishing the onset time of triggered seismicity is important both for judging statistically whether triggering has taken place (ruling out random coincidence) and for constraining physical models for remote triggering. The apparent onset (time of the first detected earthquake after Landers) varied from 30 s after passage of the Landers S wave to 33 hours after the Landers mainshock (Fig. 3 and Table 1). In general, the recognized onset time depends on the local rate of seismicity and the sensitivity of the seismic network, both of which vary regionally. Using the earthquake catalog data, we tested the hypothesis that the observed onset of activity at each site is consistent with an instantaneous increase in local seismicity rate at the time of the Landers mainshock (*15*). We were unable to reject the hypothesis at all but one of the sites, a result consistent with a causal link between the Landers earthquake and the remote earthquake activity.

The strong direct waves and the reflected and scattered coda waves produced by the mainshock and its large aftershocks tended to obscure the onset time of the triggered activity. Our approach to this problem takes advantage of the observation that seismic waves from nearby earthquakes are relatively rich in high-frequency energy, whereas waves from the Landers mainshock, having traveled a long distance, are relatively depleted in high-frequency energy as a result of intrinsic attenuation and scattering. Applying a 5- to 30-Hz bandpass filter to seismograms effectively eliminates the mainshock coda waves at distances beyond 500 km and enhances the local earthquakes (Fig. 5). The result shows that in Long Valley caldera ($\Delta$ = 415 km) and the Geysers ($\Delta$ = 740 km) the triggered activity began 30 to 40 s after the arrival of the S wave from the Landers earthquake and during the passage of the large-amplitude Love and Rayleigh surface wave trains (*16*). No evidence for such early activity was found at Parkfield, the White Mountains, Mono Basin, western Nevada, Lassen, Cedar City, Burney, or Yellowstone. Inadequate station coverage or severe signal clipping made this analysis impossible at other sites (Table 1).

It is possible that the increased seismicity rate at some sites is merely coincidental (having no causal link) with the Landers earthquake. Although the post-Landers surge in seismicity is unusual at each site, all of the sites are seismically active and have had seismicity surges (swarms) in the past (see, for example, the swarm on day 35 at Lassen Peak in Fig. 3). Considering the relative infrequency of these seismicity surges, however, noncausal coincidence is unlikely for the post-Landers activity (*17*).

Although the maximum magnitude of triggered earthquakes at each site generally decreased with distance from Landers, the duration of the triggered activity at a given site showed no clear correlation with distance (Figs. 3 and 6 and Table 1). At Long Valley and the Geysers, where seismicity is normally high, the triggered seismicity occurred as smooth transient surges in seismicity with durations of a few days and a few hours, respectively (Fig. 6), whereas at Mono Basin and Burney, triggered activity showed little sign of diminishing after 3 weeks or more (Fig. 3). The increase in number of events after the Landers earthquake varied widely from site

**Table 1.** Summary of earthquake data and modeling results for selected regions. The epicentral distances expressed in source lengths reflect the 74 km of surface faulting observed in the mainshock. Static stress changes reflect maximum shear stress change on optimally oriented planes. Daily tidal stress variation is approximately $2 \times 10^{-2}$ bar. The triggered seismicity in each region is characterized, using data in regional earthquake catalogs, by the maximum magnitude earthquake during the first 7 days after the Landers mainshock, and the numbers of events during the 7 days before ($N_b$, 21 to 28 June) and after ($N_a$, 28 June to 5 July) the Landers mainshock. Timing of the triggered activity is characterized by the interval $T_1$ between the Landers mainshock and the first located post-Landers earthquake, and by the mean interevent time $T_m$ of the first ten local earthquakes in the post-Landers activity.

| Region | Approximate distance | | Static stress change | | Max. mag. | $N_b$ | $N_a$ | $T_1$ (hr) | $T_m$ (hr) |
|---|---|---|---|---|---|---|---|---|---|
| | (km) | Source lengths | (bar) | Fraction of tidal | | | | | |
| Coso–Indian Wells | 165–205 | 2.2–2.8 | $2 \times 10^{-2}$ to $6 \times 10^{-2}$ | 1 to 3 | 4.4 | 4 | 44 | 8.6 | 4.6 |
| Little Skull Mt | 240 | 3.2 | $2.8 \times 10^{-2}$ | 1.4 | 5.6 | 10 | 59 | 1.5 | 0.9 |
| Death Valley | 300 | 4.1 | $8.0 \times 10^{-3}$ | 0.4 | 3.6 | 6 | 11 | 5.3 | 12.4 |
| White Mts* | 380–420 | 5.1–5.7 | $2.3 \times 10^{-3}$ to $3.0 \times 10^{-3}$ | 0.13 | 3.7 | 0 | 27 | 11.6 | 12.0 |
| Parkfield* | 410 | 5.5 | $6.9 \times 10^{-3}$ | 0.35 | | 8 | 11 | | |
| Long Valley* | 415 | 5.6 | $2.8 \times 10^{-3}$ | 0.14 | 3.4 | 38 | 340 | 0.15 | 0.052 |
| Mono Basin* | 450 | 6.1 | $1.9 \times 10^{-3}$ | 0.10 | 3.1 | 3 | 12 | 19.1 | 12.0 |
| Cedar City* | 490 | 6.6 | $3.6 \times 10^{-3}$ | 0.18 | 4.1 | 0 | 39 | 0.65 | 1.3 |
| Western NV* | 450–650 | 6.1–8.8 | $0.6 \times 10^{-3}$ to $2.0 \times 10^{-3}$ | 0.03 to 0.1 | 4.0 | 58 | 504 | 0.15 | 0.10 |
| Geysers*† | 740 | 10.0 | $8.7 \times 10^{-4}$ | 0.04 | 1.6 | 70 | 60 | 0.05 | 0.01 |
| Lassen* | 840 | 10.9 | $3.9 \times 10^{-4}$ | 0.02 | 2.8 | 0 | 14 | 0.2 | 5.4 |
| Burney* | 900 | 12.4 | $2.9 \times 10^{-4}$ | 0.015 | 2.8 | 1 | 9 | 23.0 | 21.0 |
| Cascade, ID | 1100 | 14.9 | $2.5 \times 10^{-4}$ | 0.01 | 1.7 | 0 | 38 | 33.3 | 1.2 |
| Yellowstone* | 1250 | 16.9 | $2.3 \times 10^{-4}$ | 0.01 | 2.1 | 0 | 16 | 1.8 | 2.1 |

*Denotes region where high-pass filtering of seismograms was used to search for early events in the Landers coda. †At the Geysers, $N_a$ and $N_b$ reflect Calnet data; $T_1$ and $T_m$ reflect Unocal data.

to site and was apparently unrelated to distance from Landers.

**Supporting observations.** Observations of both permanent and dynamic strain changes at sites of remotely triggered seismicity help constrain possible triggering processes. Of all the sites showing triggered activity, however, only Long Valley caldera has a continuous instrumental record of deformation. Data from daily measurements of a two-color geodimeter network showed no strain changes above the resolution of about 0.3 microstrain (*18*). Continuous data from a 200-m-deep borehole dilatometer 4 km west of the caldera showed an instantaneous compressional strain step of about $3 \times 10^{-9}$ between the Landers P and S waves followed by a slower compressional pulse that built to about $2 \times 10^{-7}$ during the 5 days after the mainshock. The strain pulse then decayed to background during the next few weeks (Fig. 6). Dilatometers along the San Andreas fault (solid triangles in Fig. 7) showed only an instantaneous strain step.

Information on dynamic stresses comes from on-scale records of the Landers mainshock recorded on both broad-band digital seismometers and dilatometers [Table 1; (*19*)]. The dilatometers provide a direct measurement of dilatational strain, $\theta$, and the associated dynamic mean stresses are $\sigma \approx k\theta$, where $k$ is the bulk modulus. The seismometers provide data on particle velocities, which are proportional to dynamic stresses (*20*). Peak particle velocities and dilatational strains (and thus peak dynamic stresses) occur within the S wave coda at distances beyond about 300 km and include early parts of the fundamental mode Rayleigh and Love wave trains, with dominant periods of 5 to 20 s.

The distribution of peak dynamic stresses from the Landers mainshock (Fig. 7) shows a strong directivity effect associated with the northward propagation of the mainshock rupture. Peak dynamic stresses north-northwest of the mainshock were roughly twice those at comparable distances to the west and over three times those to the south. For example, at $\Delta \approx 410$ km the peak dynamic stress was 1 to 2 bars at Parkfield but 3 to 4 bars in Long Valley caldera. Peak dynamic stresses in the San Francisco Bay area produced by the Landers mainshock (1.2 to 1.5 bars) were roughly twice those produced by the **M** = 7.1 Petrolia (Cape Mendocino) earthquake (0.5 to 0.6 bars), even though the distance from the Bay area to Landers is nearly twice that to Cape Mendocino.

Well-aquifer systems can behave as band-limited volume strain meters, and the response of such systems to the dilatational strains of Rayleigh waves from distant earthquakes is well documented (*21*). Data from water wells at Yucca Mountain (25 km northwest of Little Skull Mountain) and Long Valley caldera show pronounced transient fluctuations (amplitudes from less than 1 cm to several meters) associated with seismic waves from the Landers mainshock but no clear evidence for static offsets in local water table levels (*22*).

**Remote triggering by other large (M ≥ 6.5) earthquakes?** It might at first appear from the paucity of examples in the literature that the triggering of remote seismicity by large earthquakes is exceptional. The activity triggered by the Landers earthquake, however, consists largely of small ($M \leq 3$) events in relatively remote areas, and, as noted above, the ability to recognize reliably this level of seismic activity dates only from the late 1970s with the deployment of dense, telemetered seismic networks and computer-based, real-time data processing systems (*23*). Indeed, to search for evidence of remote triggering in the past, we must consider progressively larger (and thus less common) earthquakes, which in turn presses the issue of statistical significance.

Four other **M** ≈ 7 earthquakes have occurred in the western United States since 1980: the **M** = 7.4 Eureka, California, earthquake (located 50 km west of Cape Mendocino) of 8 November 1980; the **M** = 6.9 Borah Peak, Idaho, earthquake of 28 October 1983; the **M** = 6.9 Loma Prieta, California, earthquake of 18 October 1989; and the **M** = 7.1 Petrolia, California, earthquake of 25 April 1992. However, with the possible exception of minor swarm activity at the Geysers geothermal field coincident with the 1989 Loma Prieta and 1992 Petrolia earthquakes (distances of 220 and 230 km from the Geysers, respectively), none of these **M** ≈ 7 earthquakes appears to have triggered remote seismicity (*24*). The 1980 Eureka earthquake was essentially the same size as the Landers earthquake (both with seismic moments $M_0 \approx 1 \times 10^{27}$ dyne-cm). The other three events were smaller by factors of 2 to 3, with seismic moments ranging from $M_0 = 3.0 \times 10^{26}$ (Loma Prieta) to $M_0 = 4.5 \times 10^{26}$ dyne-cm (Petrolia). Neither the 1980 Eureka nor the 1992 Petrolia earthquakes near Cape Mendocino triggered seismicity in the vicinity of the southern Cascade volcanoes (distances 200 to 250 km), whereas the Landers earthquake, which occurred just 64 days after the Petrolia event, did trigger activity in the southern Cascades ($\Delta$ = 840 to 900 km). The Eureka and Petrolia ruptures propagated to the southwest and west, respectively (away from the continental United States), whereas the Landers rupture propagated to

the north and in the direction of the triggered activity. In any case, it appears that remote triggering requires more than simply the occurrence of a $\mathbf{M} \geq 7.3$ (or $M_0 \geq 1 \times 10^{27}$ dyne-cm) earthquake.

Remote triggering may have occurred after the 1906 San Francisco $M_s$ = 8¼ ($\mathbf{M}$ = 7.7) earthquake. Eight felt earthquakes occurred during the first 2 days within 700 km of San Francisco; most notable was a $M_s$ = 6.2 event in the Imperial Valley 11 hours after the mainshock. Similarly, seven M = 2 to 3 events near Riverside, California (distance 100 km), occurred within the first 6 hours after the $\mathbf{M}$ = 7.5 1952 Kern County earthquake. If the Imperial Valley and Riverside events were triggered, the triggering is not very remote, as they lie within 2 and 2.5 rupture lengths from their respective mainshock sources.

Two additional candidates for remote triggering involve an abrupt seismicity increase in Rabaul caldera (Papua New Guinea) on 10 May 1985 following a $M_s$ = 7.2 earthquake in New Britain 180 km away (*25*) and a swarm of some 30 locally felt earthquakes on Kyushu, Japan, that began about 16 min after the great ($M_s$ = 8) Nankaido earthquake of 21 December 1946 at a distance of 450 km (*26*). In both cases, the putative triggered activity occurred in close association with sites of young volcanism and geothermal activity.

**Triggering mechanisms.** Competitive models for the remote triggering process fall into two broad classes: One involving the static stress changes in the crust produced by the dislocation along the Landers rupture surface and the other involving the dynamic stresses associated with the propagating seismic waves generated by abrupt slip along the rupture surface. In both, remote triggering involves brittle slip on local, favorably oriented faults induced by an incremental change in the local stress field sufficient to overcome frictional strength or an incremental reduction in effective frictional strength.

Static stress changes decrease rapidly with distance (as $r^{-3}$, compared with $r^{-2}$ and $r^{-3/2}$ for dynamic stresses associated with body and surface waves, respectively) for a dislocation in an elastic half space. Maximum static shear stress changes calculated for the Landers earthquake, for example, fall below daily tidal stress changes (*27*) at distances beyond about 250 to 300 km (Table 1 and Fig. 7). The dilatational component of the static strain change calculated with this model for the vicinity of Long Valley caldera ($\Delta$ = 415 km) agrees in both sense and magnitude with the $\sim 3 \times 10^{-9}$ compressional strain step detected by the borehole dilatometer in the caldera. The small size of both theoretical and observed static stress (or strain) changes for the Landers mainshock at distances beyond about 250 km argues against their efficacy as a triggering mechanism for this instance of remote seismicity (*28*).

The relatively large, northward-directed dynamic stresses associated with the shear-wave coda and the fundamental mode Love and Rayleigh waves (Fig. 7) admit several possible mechanisms for the triggering process. In principle, an S wave (or Love wave) polarized in the plane of maximum tectonic shear stress could trigger slip on favorably oriented faults that were close to the failure threshold. S waves or Love waves propagating through a locally heterogeneous stress field will generate particle accelerations in the direction of propagation and transient stresses normal to the shear plane (*29*). The combination would facilitate slip on an optimally oriented fault by temporarily reducing the normal stress acting across the fault plane. Nonlinear constitutive laws for fault friction (*30*) admit the possibility that the frictional strength of faults can be lowered as the fault planes are worked by the dynamic strains of the passing wave field, thereby triggering slip on faults near the failure threshold.

The interaction of the dilatational component of Rayleigh waves with fluids in the crust may contribute to remote triggering. Peak dynamic stresses associated with the Rayleigh and Love wave at mid-crustal depths were on the order of a few bars at distances of at least 500 km north of the mainshock epicenter (Fig. 7 and Table 1) (*20*). Water levels in wells tapping unconfined aquifers can fluctuate greatly during the passage of Rayleigh waves from a large, distant earthquake (*21*). Where crustal fluids are confined, a passing crustal Rayleigh wave will alternately elevate and depress local pore pressure over periods of 5 to 20 s. Seismicity may be directly triggered by the compressional phase of the passing Rayleigh wave as elevated pore pressures reduce the effective strength of local faults. Indirect triggering may occur if the dynamic stresses and pore pressure transients rupture fluid seals. Previously isolated fluids would then flow into adjacent volumes with lower pressure, thereby increasing the pore pressure and decreasing effective strength in these volumes (*30a*). In this case, the onset of triggered seismicity would follow passage of the Rayleigh wave with a delay governed by local permeability, ambient pore pressures, and shear stresses.

Hot (and weaker) areas of the crust associated with young magmatic systems and geothermal areas may be particularly susceptible to the latter process because (i) rocks in the plastic domain (temperatures above 350° to 400°C), which tend to have low permeabilities and pore pressures that are near lithostatic values (*31*), may exist at relatively shallow depths and (ii) deformation in the overlying brittle (seismogenic) domain tends to be dominated by strike-slip to normal faulting (a horizontal least principal stress) such that fluid-filled cracks are vertical. This combination is favorable for the upward flow of high-pressure pore fluids from the plastic domain into the brittle crust.

More speculatively, the large dilatational strains associated with Rayleigh waves interacting with magma bodies in the upper crust may accelerate the exsolution of volatile components and temporarily increase pressure within the magma body or pore pressures in overlying rock as a result of an increased flux of volatiles out of the magma body (*32*). Alternatively, crustal magma bodies that are predominately crystalline with only a small melt fraction behave as solids rather than as liquids at small strain levels (that is, they transmit shear waves). If the large dynamic strains associated with the surface waves caused such a magma chamber to liquify partially, it would release differential stress. The resulting load transfer to the surrounding crust could trigger earthquakes in much the same way that stress redistribution in an earthquake triggers aftershocks.

Possibly, several processes contributed to the observed triggering, with the dominant process at a given site determined by the local crustal environment and location (both distance and azimuth) with respect to the mainshock source. The close association of most sites of triggered activity with recent volcanism and geothermal systems, for example, suggests that the interaction of the dilatational components of the strain field from the Landers earthquake with geothermal fluids or crustal magma bodies may be an important triggering process. At Long Valley caldera, the close temporal association between seismicity rate and the increasing part of the transient compressional strain pulse (Fig. 6) strongly points to an increase in fluid pressure somewhere in the upper crust driving the triggered seismicity.

The observation that the triggered activity persisted hours to 1 week or more after seismic waves from the Landers event subsided (and in many cases may not have begun until after the seismic waves had subsided) emphasizes that the triggered activity was not driven solely by the dynamic stresses. Whatever the triggering processes, the results were a cascading failure sequence (earthquake swarm) in crustal volumes already loaded to a critical stress state (*33*). The form and duration of individual triggered sequences are probably influenced by the same factors (the degree and characteristic dimension of fracturing, pore pressure, permeability, and so forth) that influence

the evolution of an aftershock sequence.

The observations of remote triggering of seismicity after the Landers earthquake focus attention on the nature of earthquake-fault interaction and the mechanics of the seismogenic crust. Although static-elastic dislocation models in homogeneous media may account for the occurrence of aftershocks within one to two rupture lengths from a fault, the predicted static stress changes at greater distances seem to be too small to explain remote triggering. The temporal form and spatial distribution of the remote triggering point, instead, to a class of explanations involving critically loaded faults in a heterogeneous crust, static strain amplification within weak boundaries (fault zones) between crustal blocks, and nonlinear interactions between dynamic stresses in seismic waves and crustal fluids. Although no single model seems capable of explaining all the triggered activity following the Landers earthquake, this general class of explanations is appealing because it involves geologically more realistic crustal models than does the classical, homogeneous view.

## REFERENCES AND NOTES


1. H. Kanamori, H.-K. Thio, D. Dreager, E. H. Hauksson, *Geophys. Res. Lett.*, in press. In this article we use **M** for moment-magnitude [T. Hanks and H. Kanamori, *J. Geophys. Res.* **84**, 2348 (1979)], $M$ for local network magnitudes based on either amplitude or coda duration measurements, and $M_s$ for surface wave magnitude.
2. Earthquake data used in this study were provided by regional seismograph networks operated by the U.S. Geological Survey, the California Institute of Technology, the University of Nevada, the University of Utah, the University of Washington, Boise State University, the University of Texas at El Paso, New Mexico Tech, the Idaho National Engineering Laboratory, Los Alamos National Laboratory, the Montana Bureau of Mines and Geology, the Centro de Investigación Científica y de Educación Superior de Ensenada, B.C., Mexico, the Unocal Corporation, the U.S. Bureau of Mines, and the Montana Bureau of Mines and Geology.
3. The source dimension of an earthquake is usually defined as the maximum linear measure of fault surface that slipped. The source dimension of the Landers earthquake is approximately 70 km. For comparison, the source dimension of a $M \approx 3$ earthquake (generally the smallest earthquake to produce locally felt shaking) is a few hundred meters, while that of a great (**M** ≥ 8) earthquake is a few hundred kilometers.
4. C. Kisslinger, *Eng. Geol.* **10**, 85 (1976).
5. R. A. Harris and R. W. Simpson, *Nature* **360**, 251 (1992); P. A. Reasenberg and R. W. Simpson, *Science* **255**, 1687 (1992); R. S. Stein and M. Lisowski, *J. Geophys. Rev.* **88**, 6477 (1983); K. W. Hudnut, L. Seeber, J. Pacheco, *Geophys. Res. Lett.* **16**, 199 (1989); R. S. Stein, G. C. P. King, J. Lin, *Science* **258**, 1328 (1992).
6. K. Sieh *et al.*, *Science* **260**, 171 (1993).
7. We take the southern margin of the Great Basin as defined by the belt of pronounced geophysical anomalies that cut across the southern tip of Nevada the between 36.5° and 37°N (the dashed line in Figs. 1 and 2). These coincidental anomalies include pronounced gravity and topographic gradients and the southern Nevada transverse seismic belt [G. P. Eaton, R. R. Wahl, H. J. Prostka, D. R. Mabey, M. D. Kleinkopf, *Geol. Soc. Am. Mem.* **152**, 51 (1978), R. S. Smith and M. L. Sbar, *Geol. Soc. Am. Bull.* **85**, 1205 (1974).]
8. R. E. Wallace, *J. Geophys. Res.* **89**, 5763 (1984).
9. Maps showing the distribution of geothermal areas and late Cenozoic volcanic centers are found in L. J. P. Muffler, Ed., *U.S. Geol. Surv. Circ.* **790** (1979) and R. G. Luedke and R. L. Smith, *U.S. Geol. Surv. Misc. Inv. Ser. MAP I-1091B* (1978) and *Map I-1091C* (1981), respectively; S. Hecker, *Utah Geol. Surv. Bull.*, in press; B. D. Turin, D. Champion, R. J. Fleck, *Science* **253**, 654 (1991).
10. A small swarm occurred in the Brawley seismic zone beginning a week after the Landers mainshock. This swarm appears in Fig. 2 as a cluster of epicenters in the Imperial Valley (IV).
11. J. D. VanWormer and A. S. Ryall, *Bull. Seismol. Soc. Am.* **70**, 1557 (1980); A. M. Rogers, S. C. Harmsen, E. J. Corbett, D. M. dePolo, K. F. Priestley in *Neotectonics of North America*, D. B. Slemmons, E. R. Engdahl, M. D. Zoback, D. D. Blackwell Eds. (Geological Society of America, Denver, 1991), pp. 153–184. This zone is also known as the eastern California–central Nevada seismic belt [D. P. Hill, R. E. Wallace, R. S. Cockerham *Earthquake Predict. Res.* **3**, 571 (1985)] and the eastern California shear zone [R. K. Dokka and C. J. Travis, *Tectonics* **9**, 311 (1990)].
12. J. B. Rundle and D. P. Hill, *Annu. Rev. Earth Planet. Sci.* **16**, 251 (1988). R. A. Bailey and D. P. Hill, *Geosci. Can.* **17**, 175 (1990).
13. R. B. Smith and W. J. Arabaz, in *Neotectonics of North America*, D. B. Slemmons, E. R. Engdahl, M. D. Zoback, D. D. Blackwell, Eds. (Geological Society of America, Denver, 1991), pp. 185–222.
14. In addition, less certain observations include a swarm of $M \geq 1.7$ events near Wallace, Idaho ($\Delta$ = 1400 km), beginning 4 days after the Landers earthquake [P. Swanson, personal communication] and three $M$ = 2 to 3 events in southeastern Oregon near Crump's Hot Springs ($\Delta$ = 940 km).
15. We defined the onset delay $T_1$ at each site as the time interval between the Landers mainshock and the first detected post-Landers earthquake. We represented the post-Landers seismicity at each site by a Poisson process and estimated its rate, $\lambda$, from the first ten events located at that site. Interevent times in a Poisson process are expected to exceed $3/\lambda$ 5 percent of the time. $T_1$ was less than $3/\lambda$ at all but one of the sites tested: the swarm near Cascade, Idaho, was the exception (see Table 1).
16. Before transforming the seismograms to the frequency domain, we applied a 20% cosine taper in the time domain. In the frequency domain cosine tapers were applied between 4 and 5 Hz and 30 and 35 Hz. Between 5 and 30 Hz the filter was flat.
17. We have not attempted to test the hypothesis that a regional strain event acted as a common trigger to both the Landers mainshock and the remote seismicity. Two observations stand against this hypothesis, however: (i) The Parkfield and Long Valley borehole dilatometers showed no evidence for a regional strain event before the Landers mainshock and (ii) in no case did triggered seismicity begin before the shear wave arrival from the Landers mainshock.
18. J. Langbein, *J. Geophys Res.* **94**, 9453 (1989).
19. The Landers mainshock did not trigger strong-motion seismometers at distances beyond about 200 km [A. Shakal, *CSMIP Strong-Motion Records from the Landers, California Earthquake of 28 June 1992* (*Rep. OSMS 92-09*, California Department of Conservation, CDMG, Sacramento, 1992)].
20. The relation between mean stress, $\bar{\sigma}$, and dilatational strain is $\bar{\sigma} = k\theta$, where $\bar{\sigma} = 1/3(\sigma_{11} + \sigma_{22} + \sigma_{33})$. The stress tensor for a plane shear wave has the form $\mathbf{T} = -\dot{\mathbf{u}}(\mathbf{x},t)\,(\mu/\beta)\,[\hat{\mathbf{b}}\hat{\mathbf{k}} + \hat{\mathbf{k}}\hat{\mathbf{b}}]$, where $\hat{\mathbf{k}}$ and $\hat{\mathbf{b}}$ are unit vectors in the propagation and polarization directions, respectively, $\dot{\mathbf{u}}(\mathbf{x},t)$ is particle displacement, $\mu$ is the shear modulus, and $\beta$ is shear velocity. Taking values appropriate for mid-crustal depths (Poisson ratio = 0.25, $\mu = 3.3 \times 10^{11}$ dyne cm$^{-2}$, $\rho = 2.7$ gm cm$^{-3}$, and $\beta = 3.5$ km s$^{-1}$ gives $|\mathbf{T}| \approx c\dot{\mathbf{u}}(\mathbf{x},t)$ bars, where $c \approx 1$ (bar s cm$^{-1}$). Note that the relation between dynamic stress and particle velocity does not depend on frequency for harmonic plane waves [J. N. Brune, *J. Geophys. Res.* **75**, 4997 (1970).]
21. R. C. Vorhis, in *The Great Alaskan Earthquake of 1964: Hydrology* (*Publ. 1603*, National Academy of Sciences, Washington, DC, 1968). L.-B. Liu, E. Roeloffs, X.-Y. Zheng, *J. Geophys. Res.* **94**, 9453 (1989).
22. M. L. Sorey, personal communication; G. M. O'Brian and P. Tucci, *Eos* **73**, 157 (1992).
23. E. R. Engdahl and W. A. Rinehart, in *Neotectonics of North America*, D. B. Slemmons, E. R. Engdahl, M. D. Zoback, D. D. Blackwell, Eds. (Geological Society of America, Denver, 1991).
24. The interval between eruptions of the Old Faithful geyser in Calistoga, California (30 km south-southwest of the Geysers geothermal field), also seems to be sensitive to large ($M \geq 5.5$), regional earthquakes [P. G. Silver and N. J. Valette-Silver, *Science* **257** 1363 (1992)]. The Calistoga geyser, however, failed to respond to the Landers mainshock (P. G. Silver, personal communication).
25. J. Mori *et al.*, in *Volcanic Hazards: Assessment and Monitoring*, J. H. Latter, Ed. (Springer-Verlag, Berlin, 1989), pp. 429–462.
26. K. Abe, personal communication.
27. Peak stresses due to the solid Earth tides typically range from 0.01 to 0.03 bar (strains in the range 0.02 to 0.06 microstrain). Peak tidal stresses the day of the Landers mainshock were about 0.02 bar (0.04 microstrain).
28. The possibility remains, however, that static or quasi-static stress changes may result in delayed triggering of earthquakes over a time scale of months to years as co-seismic stresses in the lower crust and asthenosphere relax and transfer load to the overlying seismogenic crust, which may, in turn, concentrate stress in relatively weak faults. The ability of static strain changes within weak zones to trigger local seismicity may be further enhanced if the weak zones are relatively impermeable such that the strain changes drive large changes in local pore pressure [J. R. Rice and J.-C. Gu, *Pure Appl. Geophys.* **121**, 187 (1983); S. C. Jaumé and L. R. Sykes, *Science* **258**, 1325 (1992); M. L. Blanpied, D. A. Lockner, J. D. Byerlee, *Nature* **358**, 574 (1992).
29. C. Kisslinger and J. T. Cherry, *Eos* **51**, 353 (1970).
30. P. Okubo and J. H. Dieterich, in *Earthquake Source Mechanics*, S. Das, J. Boatwright, C. Scholz, Eds. (American Geophysical Union, Washington, DC, 1986), pp. 37–48.

30a. J. Byerlee, *Geology* **21**, 303 (1993).

31. R. O. Fournier, *Geophys. Res. Lett.* **18**, 955 (1991).
32. R. I. Tilling, J. M. Rhodes, J. W. Sparks, J. P. Lockwood, P. W. Lipman, *Science* **235**, 196 (1987); D. L. Sahagiam and A. A. Proussevitch, *Eos* **73**, 627 (1992).
33. In the terminology of nonlinear dynamics, the sites that responded to the Landers earthquake with triggered seismicity had reached a state of self-organized criticality sometime before the Landers earthquake, with a correlation length spanning much of the Great Basin [see, for example, J. B. Rundle, in *Chaotic Processes in the Geological Sciences*, D. A. Yuen, Ed. (Springer-Verlag, Berlin, 1992), pp. 293–303].
34. Y. Okada, *Bull. Seismol. Soc. Am.* **82**, 1018 (1992).


35. We thank J. Savage, P. Spudich, T. Hanks, R. Aster, P. Silver, and an anonymous referee for their helpful comments in review.

8 February 1993; accepted 3 May 1993